23RD EUROPEAN ROTORCRAFT FORUM 1997

PROCEEDINGS - VOLUME TWO

16-18 September 1997
Dresden, Germany

Published by DGLR, Godesberger Allee 70,
D-53175 Bonn, Germany

XV-15 AEROACOUSTIC TESTING AT NASA AMES

Jeffrey S. Light Cahit Kitaplioglu C.W. Acree

NASA Ames Research Center
Moffett Field, California

Abstract

Two tests were completed by NASA Ames Research Center to measure the acoustics and performance of an XV-15 rotor. These tests were a flight test of the XV-15 aircraft and a wind tunnel test of a single, full-scale XV-15 rotor. Acoustics and performance measurements were obtained for helicopter-mode forward flight and descent conditions. This paper summarizes the data obtained from these tests. Comparisons are made of blade loads and acoustics data obtained from the two tests. These comparisons provide insight into both wind tunnel and flight test experimental techniques and capabilities.

Notation

C_Q	rotor torque coefficient
C_T	rotor thrust coefficient
i_N	nacelle incidence angle, deg
M_{tip}	rotor tip Mach number
R	rotor radius, ft
α_A	aircraft angle of attack, deg, positive nose up
α_S	shaft angle, deg, positive aft
α_{tpp}	rotor tip-path-plane angle, deg, positive aft
β_{1C}	longitudinal flapping angle, deg, positive aft
μ	advance ratio
σ	rotor solidity ratio
Ω	rotor rotational speed, rad/sec

Introduction

Tiltrotor aircraft hold the promise to greatly enhance the air transportation system of the future. They combine the vertical takeoff and landing (VTOL) capabilities of helicopters with high speed capabilities similar to turboprop aircraft. However, capitalizing on the tiltrotor's potential requires a greater understanding of its performance and acoustics, especially for takeoff and landing.

The XV-15 aircraft was developed in the early 1970's as a proof of concept vehicle. Performance and acoustics testing were performed during development to ensure the viability of the concept (Refs. 1-4). Environmental concerns over vertiport placement has increased the need for in-depth knowledge of tiltrotor acoustics for landing approaches (Refs. 5, 6).

Presented at the 23rd European Rotorcraft Forum, Dresden, Germany, 16-18 September 1997

Two recent tests of the XV-15 rotor system have been performed by NASA Ames, one in flight and the other in a wind tunnel. The tests were performed to measure blade-vortex interaction (BVI) noise and helicopter-mode performance and loads for the XV-15 rotor. One of the goals of these tests was to develop and validate methods of testing that provide acoustics measurements of the XV-15 rotor in the wind tunnel that match measurements made in flight.

In-flight acoustics measurements of the Bell XV-15 Tiltrotor Research Aircraft were obtained as part of the In-flight Rotorcraft Acoustics Program (IRAP). IRAP was established with the objective of acquiring in-flight acoustic data to validate wind tunnel measurements. A detailed description of IRAP is given in Ref. 7.

In addition to flight testing, a full-scale, single XV-15 rotor was tested in the National Full-Scale Aerodynamics Complex (NFAC) 80- by 120-Foot Wind Tunnel. Acoustics, performance, and loads were measured for tunnel speeds from 60 to 80 knots, and for rotor tip-path-plane angles from -15 deg to +15 deg (Refs. 8, 9).

Limited comparisons between the wind tunnel and flight test measurements for the XV-15 rotor have been performed. Previous examination of wind tunnel and flight test measurements have demonstrated the challenges involved in making these comparisons. Blade load measurements for a hingeless helicopter main rotor are known to be highly dependent on trim methods (Ref. 10). Previous studies of BVI acoustics showed acceptable comparison of wind tunnel and flight test acoustic signatures in the form of similar pulse widths and noise levels (Refs. 11, 12). However, discrepancies were noted in the shaft angle at which best agreement was obtained.

This paper summarizes results of the two tests of the XV-15 rotor system. Measurements from each test are compared, and issues associated with comparing wind tunnel measurements with tiltrotor aircraft measurements are presented.

Flight Test

IRAP testing requires two aircraft, the subject rotorcraft and the NASA YO-3A Acoustics Research Aircraft. The subject rotorcraft for this test, the XV-15 Tiltrotor Research Aircraft, consists of an airplane-style fuselage and wings, with 25-ft diameter

Table 1. XV-15 rotor characteristics.

Number of blades	3
Rotor radius	12.5 ft
Blade chord at tip	14 in
Rotor solidity	0.089
Blade twist	-41 deg (nonlinear)
Hub precone angle	1.5 deg
Rotor airfoils	NACA 64-series

rotors mounted on each wingtip. The nacelles and turbine engines rotate to vertical to provide hovering and helicopter mode flight. The nacelles rotate forward to provide propulsive force in airplane mode flight and speeds up to 300 knots. The XV-15 rotor system has three highly twisted, metal blades with a radius of 12.5 ft (Table 1). A detailed description of the XV-15 aircraft is found in Ref. 13.

The YO-3A is a low-noise airplane modified by NASA specifically for acquiring in-flight measurements of rotorcraft noise. Microphones mounted on the YO-3A wingtips and vertical tail measure noise when the airplane is flown in formation with a test rotorcraft. A detailed description of the YO-3A aircraft is found in Ref. 14. Figure 1 shows the XV-15 and the YO-3A in formation.

Flight conditions and microphone locations were selected to measure the BVI noise from the starboard rotor of the XV-15. The flight formation of the two aircraft was maintained such that the starboard wing tip microphone of the YO-3A was positioned 20 deg below the starboard rotor hub and at a rotor azimuth of 150 deg. This was the estimated radiation direction for peak BVI noise from the starboard rotor and was a location for a microphone that could be readily matched in the 80-by 120-Foot Wind Tunnel. The nominal distance between the starboard wing tip microphone and the starboard rotor hub was three rotor diameters (75 feet). The relative distance between the XV-15 and YO-3A was measured with a laser rangefinder.

Because the two rotors on the XV-15 aircraft rotate in opposite directions, BVI acoustic radiation from each rotor will be in widely separate directions. Therefore, the advancing side BVI noise of the port rotor should contribute only minimally to the BVI noise of the starboard rotor measured on its advancing side. The BVI acoustic measurement from the YO-3A microphone will essentially be equivalent to testing the starboard rotor alone. This is an important assumption when comparing the flight test and wind tunnel data for the tiltrotor configuration, and was investigated as part of the wind tunnel experiment.

Test Conditions

The range of test conditions from IRAP testing of the XV-15 aircraft are summarized in Table 2. All test flights were flown with the XV-15 in helicopter-mode, with nacelle incidence angle (i_N) nominally set to 90 deg. Steady conditions were necessary for high quality flight test data, hence low air turbulence, as assessed by the pilot, was required for each data point. Multiple data runs with the same flight conditions were flown to ensure data repeatability.

Flight Test Data Acquisition and Processing

Flight test conditions, including airspeed, tip speed, rotor torque, aircraft angle of attack, gimbal angle, and collective and cyclic control positions were measured during the IRAP flights. Blade load and control system loads were also measured. Thirty-second data records were recorded for each flight condition. All channels were low-pass filtered (50 Hz for pitch link, 100 Hz for blade bending moments) to prevent aliasing. Unlike most rotorcraft tested under IRAP, the XV-15 was instrumented to provide aircraft angle of attack and rotor gimbal angle measurements. Because the gimbaled rotor of the XV-15 is essentially rigid, the rotor tip-path-plane can be calculated ($\alpha_{tpp}=\alpha_S+\beta_{1C}$). The shaft angle is computed using the aircraft angle of attack and nacelle angle ($\alpha_S=\alpha_A-(i_n-90)$). Rotor torque was directly measured via gages on the rotor shaft.

Time histories of aircraft separation distance and trim state, as well as pilot comments, were examined to select the steadiest section of each 30-sec data record for analysis. The steadiest 32 revolutions (about 3 sec) of each data record were selected for processing.

The acoustic signal at each test condition was measured using a Bruel & Kjaer 0.5-in microphone mounted on the starboard wing of the YO-3A. Thirty seconds of acoustic data were recorded on an FM analog tape recorder, set to the IRIG Wideband I standard and operated at 30 ips (resulting in an overall 0-20 kHz frequency response and 48 dB dynamic range). A 1/rev azimuth reference transmitted from the XV-15 was also recorded.

The data were low pass filtered at 5 kHz to prevent aliasing and digitized at 2048 points/rev. The data were then time averaged based on manual

Table 2. Flight test parameters.

Parameter	Value
M_{tip}	0.69
α_{tpp}	-0.4 deg to +2.5 deg
μ	0.154 to 0.164
C_Q	0.00045 to 0.00060

selection of a repeating acoustic peak for each blade of each revolution. This technique (Refs. 11, 12) eliminated the smearing of the BVI pulse peaks caused by RPM unsteadiness in standard averaging techniques. An average acoustic pressure time history was generated for each flight condition.

Three noise level metrics were obtained by integrating the respective sound pressure power spectra: OASPL from the unfiltered spectra, dBA from the A-weighted power spectra, and BLdB from a bandpass filtered spectra. The bandpass filtering method was used to highlight BVI events. For this method, the averaged time histories were digitally filtered to attenuate frequency content below the 10th and above the 50th blade passage harmonics. This preserves the peak-to-peak amplitude and pulse width of the high amplitude acoustic pulse indicative of the BVI pulse, while effectively attenuating low frequency content unrelated to BVI (Ref. 9). The BLdB metric is used for the results presented in this paper.

Wind Tunnel Test

Wind tunnel testing was conducted in the 80- by 120-Foot Wind Tunnel of the National Full-Scale Aerodynamics Complex (NFAC) located at the NASA Ames Research Center (Fig. 2). A single, full-scale, XV-15 rotor was tested on the Ames Rotor Test Apparatus (RTA). The rotation direction of the rotor was the same as the starboard rotor from the aircraft. Figure 3 shows the model installed in the wind tunnel. The rotor system and gimbaled hub are actual aircraft hardware, with modifications made to facilitate attachment to the RTA.

The RTA is a special-purpose test stand for operating rotors in the NFAC. The RTA houses electric drive motors, a right-angle transmission, a 5-component rotor balance with 22,000 lb thrust capacity, and primary and dynamic control systems. The RTA was mounted in the wind tunnel on a three-strut support system placing the rotor hub nominally 31 ft (2.5 R) above the wind tunnel floor. The model angle of attack was changed by adjusting the height of the tail strut. This installation allowed test stand angles, and therefore rotor shaft angles, from -15 deg (forward) to +15 deg (aft). Rotor collective and cyclic pitch controls were input through the swashplate by three electro-mechanical/hydraulic actuators.

The 80-by 120-Foot Wind Tunnel test section has a sound absorbing liner which attenuates acoustic reflections down to approximately 250 Hz (absorption>90%). In addition to the liner, sound-absorbing foam was attached to portions of the RTA fuselage and other selected points to eliminate reflections from hard surfaces. This foam is partially visible in Fig. 3.

For acoustic measurements, several microphones were placed around the model as indicated in Fig. 4. Four traversing microphones (Microphone #1-Microphone #4) were placed on the advancing side of the rotor and 1.8 rotor radii below the rotor to measure the BVI noise footprint. One microphone (Microphone #5) was positioned at a distance matching the starboard wing microphone on the YO-3A aircraft as flown during IRAP flight testing. Another microphone (Microphone #6) was placed in a "mirror-image" position in the wind tunnel test section to simulate the effect of the port-side rotor of the XV-15 aircraft as measured by the YO-3A microphone. The "mirror-image" microphone was positioned at the proper angle relative to the rotor hub, but at a somewhat closer distance, as indicated in Fig. 4, due to test section constraints.

Instrumentation and Data Acquisition

The rotor hub loads were measured by the RTA rotor balance, which measures lift, drag, and side forces, together with the rotor pitching and rolling moments. Also incorporated was an instrumented flex-coupling to measure rotor torque. The rotor balance data have not been corrected for any aerodynamic hub tares. Blade loads, control system loads, and control inputs were also measured. Radial locations for the flap bending moment, chord bending moment and blade torsion measurements are shown in Fig. 5.

Data acquisition of performance and load parameters was synchronized to the rotor position, with 64 samples per revolution, and low-pass filtered at 100 Hz. Time history data are available for all channels, and have been corrected to account for amplitude and phase shifts caused by filtering.

The acoustic data were recorded and processed on a separate data system. Bruel and Kjaer 0.5-in microphones measured the acoustic signals, which were amplified, anti-alias filtered at 4 kHz, and recorded on the Acoustic Data Acquisition System (ADAS). The acoustic data were digitized with 16-bit resolution (>80 dB dynamic range) at 2048 per rev (approximately 20k samples per second). Sixteen revolutions of data were recorded at each test point. A 1/rev azimuth signal was recorded in addition to the microphone signals.

The acoustic data obtained during the wind tunnel test were averaged in the time domain with 2048 points (one revolution) per frame. Sixteen frames of data were utilized in each time average.

Table 3. Nominal wind tunnel test conditions.

M_{tip}	0.690
α_s	-15 deg to +15 deg, 1 deg increments
μ	0.125, 0.150, 0.170
C_T/σ	0.060, 0.075, 0.090, 0.105

Test Conditions and Envelope

Wind tunnel test data were established using two methods. The first method used a matrix approach, and the second sought to match specific operating conditions with the IRAP test. For the matrix approach, testing was conducted over a range of advance ratios, shaft angles, and C_T/σ's as shown in Table 3. Test conditions were reached by first setting a constant tunnel speed and then varying the rotor shaft angle while maintaining a constant C_T/σ. In general, rotor flapping, as measured by the hub gimbal angle, was trimmed to zero, so shaft angle corresponds to rotor tip-path-plane angle. Initial runs established the combination of advance ratio and tip-path-plane angle for peak BVI noise levels measured at Microphone #5. Subsequently, detailed acoustic data were obtained for values of advance ratio and tip path plane angle at and near the peak BVI conditions. This included surveys of the acoustic field below the advancing side of the rotor using the microphone traverse.

Matching wind tunnel test conditions with those measured during flight required a different approach. The rotor trim state was not matched exactly between the wind tunnel and flight test. The longitudinal flapping on the aircraft results from balancing aircraft moments for a given flight condition. These values of longitudinal flapping were not obtainable in the wind tunnel due to control system load constraints. Therefore, the rotor tip-path-plane angle ($\alpha_{tpp}=\alpha_S+\beta_{1C}$) was matched between the two tests, rather than the shaft angle and longitudinal flapping individually. As there was no direct measure of rotor thrust on the aircraft, and estimating the rotor thrust from the aircraft weight and wing lift was problematic, the rotor torque coefficient was used as a matching parameter. The rotor torque is a direct measurement from the rotor shaft for both the XV-15 aircraft and the wind tunnel model. It was assumed that by matching μ, M_{tip}, α_{tpp} and C_Q, the rotor thrust for the two tests will be matched.

Wind Tunnel Results

Performance

Rotor performance was measured for shaft angles from -15 deg to +15 deg at a constant $C_T/\sigma=0.075$, for three advance ratios (Fig. 6). As shaft angle was increased, the rotor torque coefficient decreased in a roughly linear manner for a given advance ratio. At positive shaft angles, changes in the tunnel speed result in changes in torque coefficient. However, at $\alpha_S=-15$ deg, tunnel speed has very little effect on the power required to maintain thrust. A more detailed examination of the wind tunnel results, including hover and forward flight performance, can be found in Ref. 8.

Blade Loads

Figure 7 shows the time history of the flap bending moment at 0.35R as a function of shaft angle, for $\mu=0.125$, and $C_T/\sigma=0.075$. This figure illustrates the changes in magnitude and waveform for flap bending moment over the range of shaft angles tested. The mean value of the flap bending moment decreases with increasing shaft angle. All shaft angles show similarly increasing loads on the advancing side, while differences in loading on the retreating side are apparent.

Figure 8 shows the time history of the chord bending moment at 0.35R as a function of shaft angle, for $\mu=0.125$, and $C_T/\sigma=0.075$. The waveforms and magnitude change significantly over the range of shaft angles tested.

Acoustics

Figure 9 is a plot of noise levels, measured at Microphone #5, over the range of tip-path-plane angles of attack and advance ratios tested, for a fixed $C_T/\sigma=0.075$. The figure shows that the highest noise levels occurred at α_{tpp} of approximately +4 deg (nose up) and advance ratio of 0.170.

Figure 10 demonstrates the acoustic footprint at the highest measured BVI condition ($\alpha_{tpp}=4$ deg, $\mu=0.170$, $C_T/\sigma=0.075$). Note the highest values are measured toward the starboard edge of the traverse range. Future testing will expand the traverse range to ensure this outer region is suitably measured. A more detailed examination of the BVI acoustics measured during the wind tunnel test can be found in Ref. 9.

Wind Tunnel / Flight Test Comparisons

The wind tunnel test was conducted after flight testing, providing an opportunity to match specific data points. A preliminary comparison between wind tunnel and flight test measurement has been performed. Table 4 shows the matching test condition examined in this paper. This was the closest matching condition obtained due to limitations in the control system hardware specific to the RTA test installation. Both data sets have been corrected to account for amplitude and phase shifts caused by filtering.

Loads

A comparison of the pitch-link load measurement between the wind tunnel and flight conditions is shown in Fig. 11. Both traces show a strong 1/rev component, while the wind tunnel data also have a higher frequency (9/rev) component. There are two possible explanations for this. First, the lower filter setting for the pitch link during the flight test (50 Hz,

Table 4. Matching test condition for XV-15 flight test and wind tunnel test.

	μ	α_S (deg)	β_{1C} (deg)	α_{tpp} (deg)	M_{tip}	C_Q
Wind tunnel	0.157	1.5	0.1	1.6	.690	.00044
Flight test	0.159	0.6	1.3	1.9	.690	.00045

vs. 100 Hz in wind tunnel) may be eliminating the high frequency content. Second, the stiffer control system of the RTA, compared to that of the aircraft, could account for the high frequency oscillations.

The aircraft starboard rotor and the wind tunnel rotor each had flap and chordwise bending moment gages at the 35% radial station. A comparison of the flap bending moment at 0.35R is shown in Fig. 12. Both waveforms show the 1/rev and higher frequency oscillations in flap bending moment. The significant differences in the mean values could be caused by the different trim methods used in each test. For the flight test data, the increase in flap bending moment near the wing location of 270 deg could be attributed to aerodynamic interaction with the wing. However, this same increase is seen for the wind tunnel case. This suggests that for blade loads measurements, the isolated rotor of the wind tunnel test adequately models the rotor/wing configuration of the aircraft.

The chord bending moment at 0.35R is compared in Fig. 13 for the wind tunnel and flight test conditions of Table 4. The time histories again show similar 1/rev and higher frequency oscillations. The chordwise bending moment corresponds to drag on the blade, and thus, rotor torque. Therefore, the agreement of the mean values could result from the choice of C_Q as a matching parameter. If rotor thrust coefficient were matched, rather than C_Q, it is conceivable that flap bending moment would show better agreement.

Acoustics

The time histories of acoustic pressure measured at the test conditions of Table 4 are compared in Fig. 14(a). To facilitate comparison, the flight test data have been phase shifted so that the BVI pulses align. Blade-to-blade differences are evident, as are differences in the regions between the BVI events. However, overall features of the waveforms, such as pulse width and the relative azimuth separation of maxima/minima, agree reasonably well.

Figure 14(b) shows the same time history with an expanded azimuth scale. The amplitude of the BVI event is larger for the wind tunnel data. This is consistent throughout the dataset.

Trim Considerations

Changes in shaft angle were found to affect the amplitude of the BVI occurrence. Comparison of the acoustic time history measured in the wind tunnel for shaft angles from 1.5 deg to -4 deg, showed the best amplitude match with flight test data was obtained for a shaft angle of -3 deg (Ref. 9). Figure 15 shows the acoustic time histories for the conditions of Table 4, as well as for a shaft angle of -3 deg obtained in the wind tunnel. The delay in azimuth of the pulse with the increase in α_{tpp} is consistent with the increase in distance to the measurement microphone. The sound pressure has been distance normalized to account for the change in source-microphone separation as α_{tpp} varies. Note the closer agreement in peak-to-peak amplitude for the 1.9 deg flight test and -3 deg shaft angle cases.

This comparison is carried a step further in Fig. 16, which shows the time history of the flap bending moment for the matching conditions of Table 4 and for a shaft angle of -3 deg. The -3 deg shaft angle case provides a closer match with the mean value measured in the flight test. It also shows the local peak in flap bending near 350 deg azimuth.

Figure 17 shows the time history of the chordwise bending moment for the matching conditions of Table 4 and for a shaft angle of -3 deg. It also captures the higher frequency oscillations better than the 1.6 deg case.

These results suggest limitations in the matching of the flight test and wind tunnel data. The discrepancy may arise from the tip-path-plane angle measurement in the wind tunnel or on the aircraft. The difference may also be caused by the different rotor thrust or different flapping conditions on each rotor. It must also be realized that this is based on comparisons at only one condition. Additional comparisons should be completed in order to better understand these differences.

Conclusions

Two tests were conducted by NASA Ames Research Center to examine the BVI acoustics and performance of the XV-15 rotor. A flight test of the XV-15 Tiltrotor Research Aircraft was conducted to measure the BVI acoustics of the rotor for descent flight conditions. A wind tunnel test of a single, full-scale XV-15 rotor was conducted to measure performance, loads, and acoustics for a range of shaft angles and advance ratios. Comparison between the wind tunnel and flight test results provide the following conclusions:

1) Wind tunnel and flight test time histories for pitch-link, flap bending, and chord bending loads agree reasonably well for the test condition examined.

2) Influence of RTA body in the wind tunnel test, and XV-15 wing/fuselage in flight test, has no discernible effect on blade bending loads.

3) Improved agreement of results can be obtained by matching torque coefficient and advance ratio while adjusting the tip-path-plane angle. This provides a better match of the BVI noise amplitude, as well as better matching of the details of the blade bending moments.

References

1. "Advancement of Proprotor Technology, Task 2: Wind-Tunnel Test Results," NASA CR 114363, September 1971.

2. Edenborough, H. K., Gaffey, T. M., and Weiberg, J. A., "Analyses and Tests Confirm Design of Proprotor Aircraft," AIAA Paper No. 72-803, AIAA 4th Aircraft Design, Flight Test, and Operation Meeting, Los Angeles, CA, August 1972.

3. Marr, R. L., "Wind Tunnel Results of 25-Foot Tilt-Rotor During Autorotation," NASA CR 137824, February 1976.

4. Lee, A. and Mosher, M., "An Acoustical Study of the XV-15 Tilt Rotor Research Aircraft," AIAA Paper No. 79-0612, AIAA 4th Aeroacoustics Conference, Seattle, WA, March 1979.

5. Edwards, B., "XV-15 Tiltrotor Aircraft Noise Characteristics," AHS 46th Annual Forum, Washington, DC, May 1990.

6. Conner, D., Marcolini, M., Edwards, B., and Brieger, J., "XV-15 Tiltrotor Low Noise Terminal Area Operations," AHS 53rd Annual Forum, Virginia Beach, VA, April 1997.

7. McCluer, M. and Dearing, M., "Measuring Blade Vortex Interaction Noise Using the YO-3A Acoustics Research Aircraft," 22nd European Rotorcraft Forum, Brighton, UK, September 1996.

8. Light, J., "Results of an XV-15 Test in the National Full-Scale Aerodynamics Complex," AHS 53rd Annual Forum, Virginia Beach, VA, April 1997.

9. Kitaplioglu, C., McCluer, M., and Acree, C.W., "Comparison of XV-15 Full-Scale Wind Tunnel and In-Flight Blade Vortex Interaction Noise," AHS 53rd Annual Forum, Virginia Beach, VA, April 1997.

10. Peterson, R.L., Maier, T., Langer, H.J., and Tranapp, N., "Correlation of Wind Tunnel and Flight Test Results of a Full-Scale Hingeless Rotor," AHS Aeromechanics Specialist Conference, San Francisco, CA, January 1994.

11. Yamauchi, G. K., Signor, D. B., Watts, M. E., Hernandez, F. J., and LeMasurier, P., "Flight Measurements of Blade-Vortex Interaction Noise Including Comparisons with Full-Scale Wind Tunnel Data," AHS 49th Annual Forum, St. Louis, MO, May 1993.

12. Signor, D. B., Watts, M. E., Hernandez, F. J., and Felker, F. F., "Blade Vortex Interaction Noise: A Comparison of In-Flight, Full-Scale and Small-Scale Measurements," AHS Aeromechanics Specialist Conference, San Francisco, CA, January 1994.

13. Maisel, M.A., "NASA/Army XV-15 Tilt Rotor Research Aircraft Familiarization Document," NASA TM X-62407, January 1975.

14. Cross, J.L., "YO-3A Acoustics Research Aircraft Systems Manual," NASA TM 85968, July 1984.

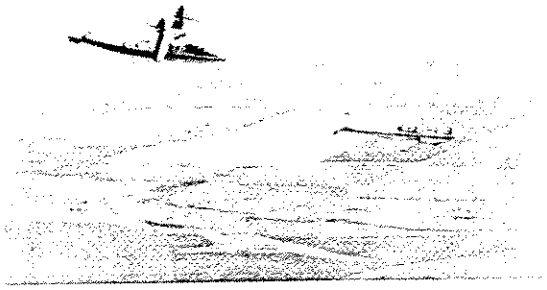

Fig. 1. XV-15 aircraft in formation flight with the YO-3A.

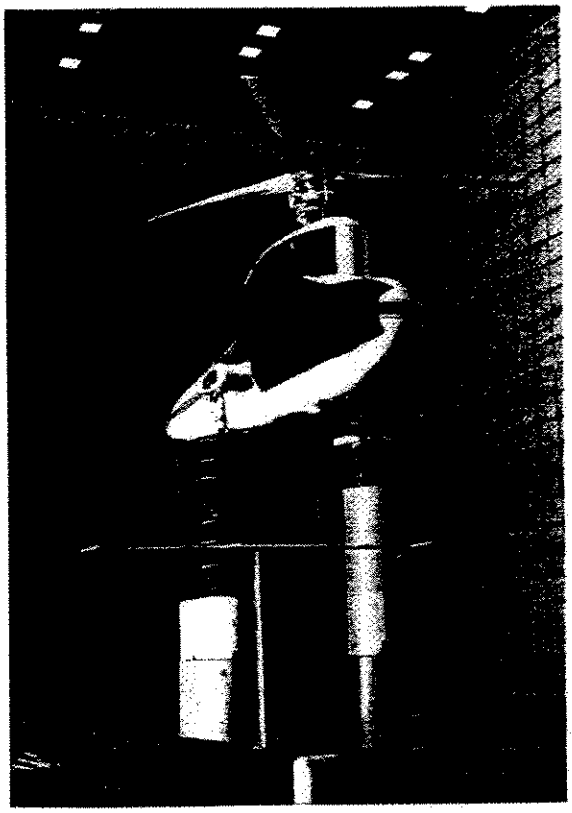

Fig. 3. XV-15/RTA test installation in the 80- by 120-Foot Wind Tunnel.

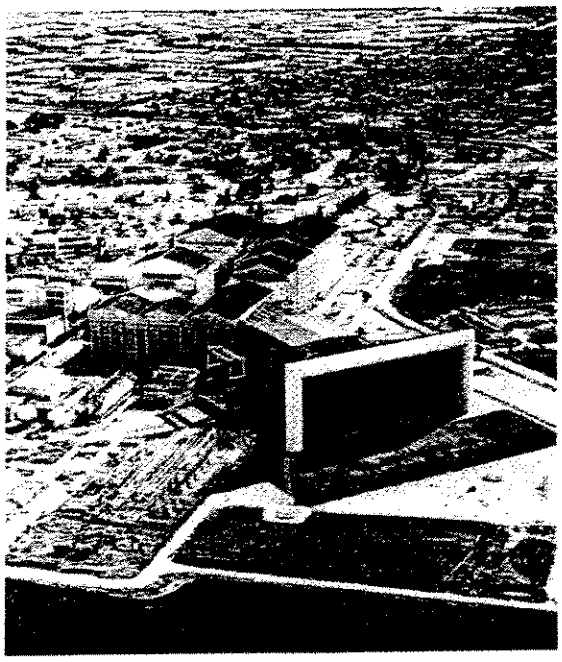

Fig. 2. National Full-Scale Aerodynamics Complex, with 80- by 120-Foot Wind Tunnel in foreground.

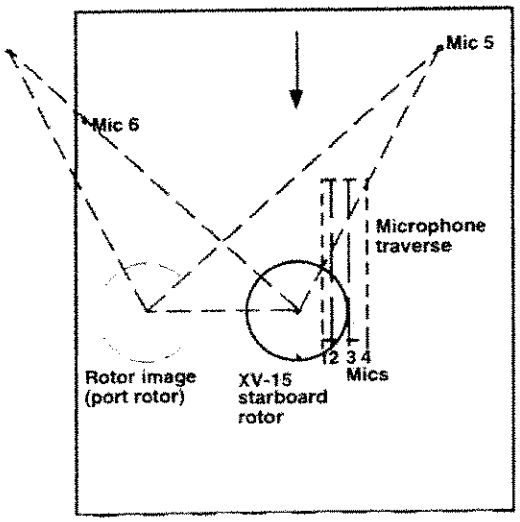

Fig. 4. Microphone locations during wind tunnel test.

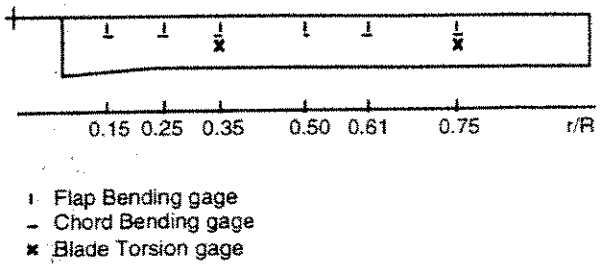

Fig. 5. Blade bending moment measurement locations on the XV-15 blade.

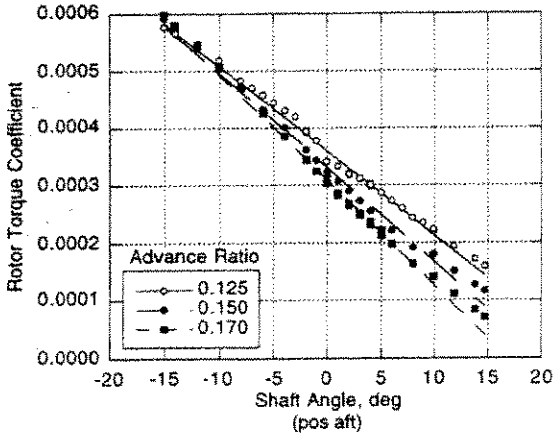

Fig. 6. Rotor torque coefficient as a function of shaft angle (C_T/σ=0.075).

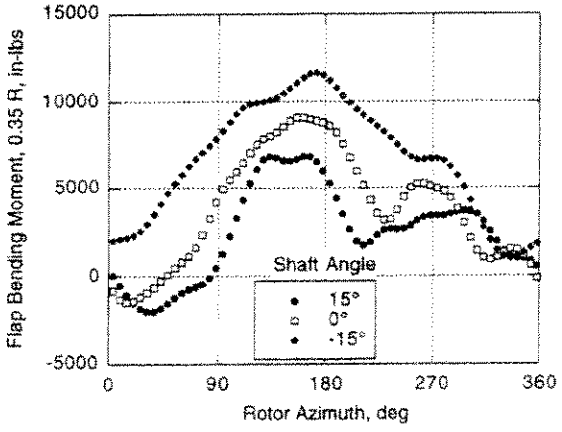

Fig. 7. Effect of shaft angle on flap bending moment, 0.35R (μ =0.125, C_T/σ=0.075).

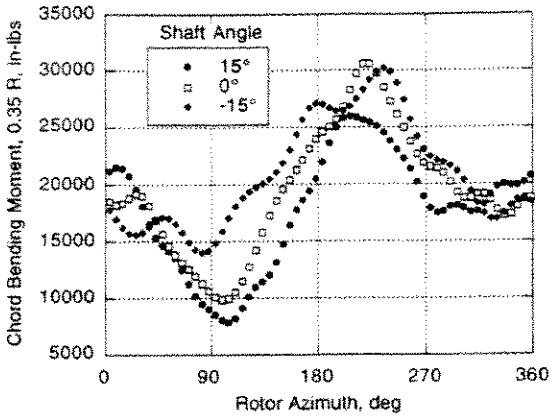

Fig. 8. Effect of shaft angle on chord bending moment, 0.35R (μ=0.125, C_T/σ=0.075).

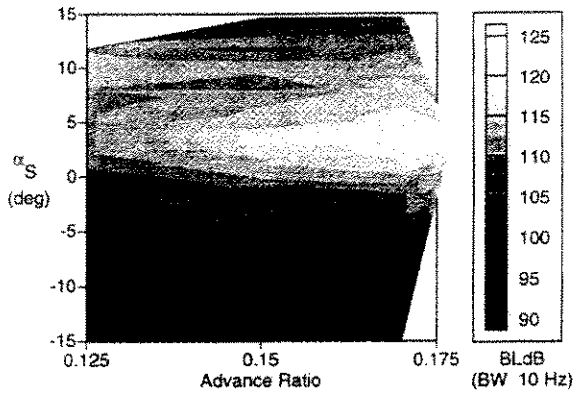

Fig. 9. XV-15 rotor acoustics measurements in wind tunnel (M_{tip}=0.690, C_T/σ=0.075, Microphone #5).

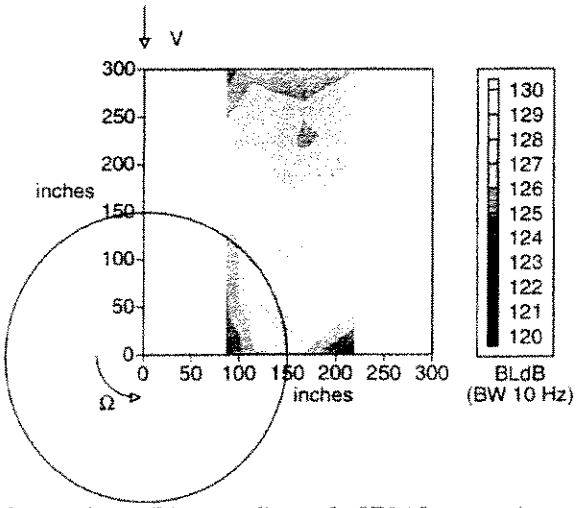

Fig. 10. Directionality of XV-15 acoustics (M_{tip}=0.690, C_T/σ=0.075, μ=0.170, α_S=4 deg).

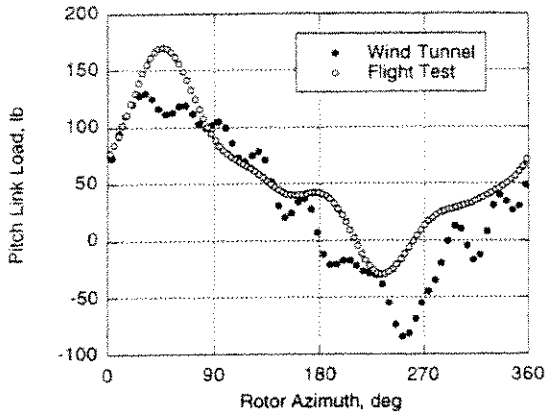

Fig. 11. Comparison of pitch-link load time history for wind tunnel and flight test.

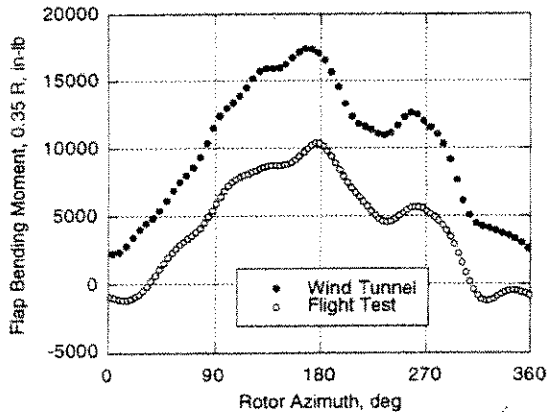

Fig. 12. Comparison of flap bending moment for wind tunnel and flight test.

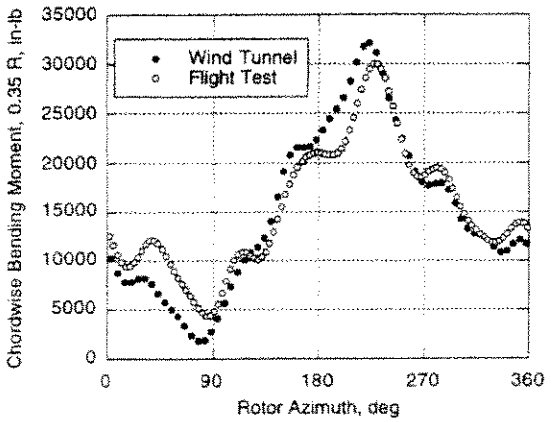

Fig. 13. Comparison of chordwise bending moment for wind tunnel and flight test.

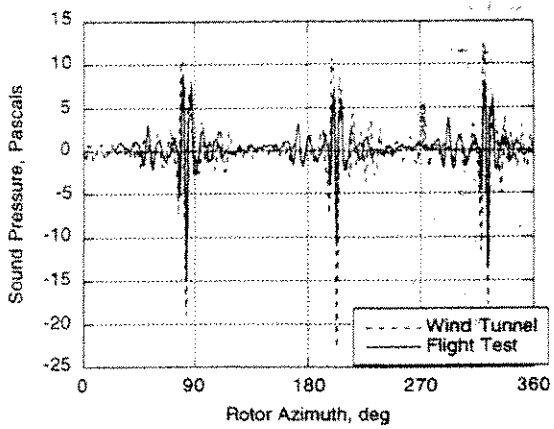

Fig. 14(a). Comparison of filtered acoustic time histories for wind tunnel and flight tests.

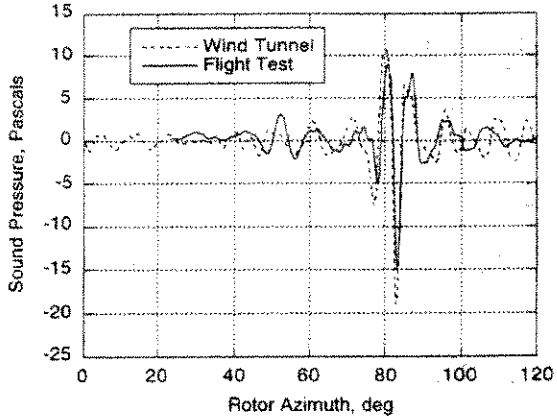

Fig. 14(b). Comparison of filtered acoustic time histories, expanded azimuth, blade 1.

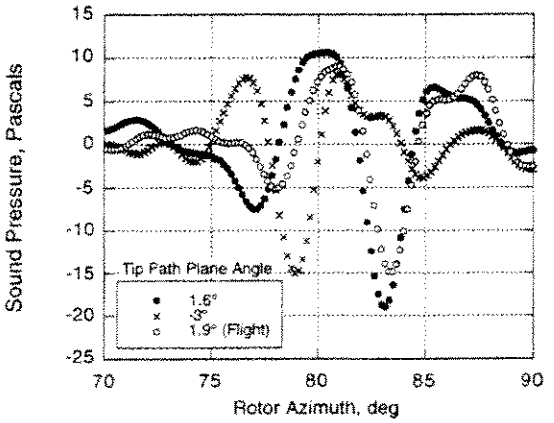

Fig. 15. Change in acoustics time history for several tip-path-plane angles (C_Q=0.00044, μ=0.157).

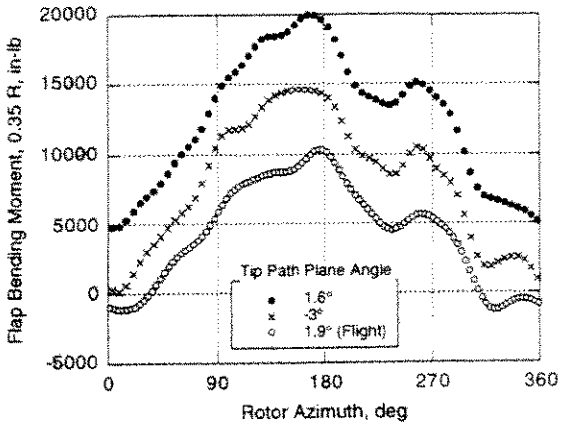

Fig. 16. Change in flap bending moment time history for several tip-path-plane angles (C_Q=0.00044, μ=0.157).

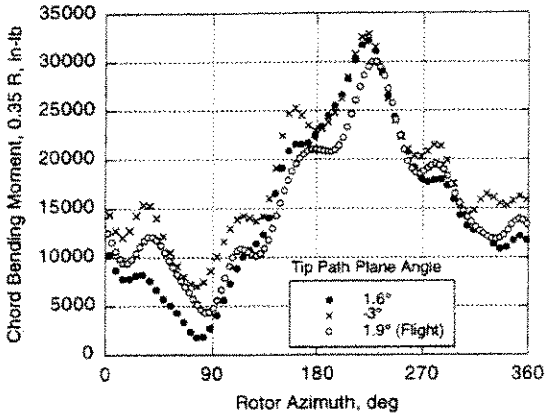

Fig. 17. Change in chord bending moment time history for several tip-path-plane angles (C_Q=0.00044, μ=0.157).